# TIME RESOLVED MEASUREMENTS OF FLUX-FLOW OSCILLATOR LINEWIDTH

U. Müller, K. Jacobs
KOSMA, I. Physikalisches Institut, University of Cologne
Zuelpicher Str. 77, 50937 Cologne, Germany

## ABSTRACT

Superconducting Flux-Flow Oscillators (FFO) as local oscillators for radio astronomy are perfectly suited to be combined with SIS-mixing-devices in standard Nb/Al-$AlO_X$/Nb technology, having the potential to result in highly sophisticated integrated receivers up to the terahertz region. Oscillator linewidth and -stability are of exceptional importance for radio astronomical applications.
A spectroscopic measurement setup for the 350GHz-band has been built up to investigate the radiation properties of superconducting oscillators. We report on unique time resolved measurements of Flux-Flow Oscillator radiation characteristics using a modified KOSMA Acousto-Optical Spectrometer (AOS). Measurements with an integration time of 1μs result in a FFO linewidth of less than 1MHz at 350GHz. A simultaneously recorded spectrum analyzer trace with a sweep time of 40ms shows a FFO-linewidth of more than 20MHz. It is concluded that the time averaged linewidth of the Flux-Flow Oscillator - as can be seen on the spectrum analyzer - is due to frequency modulation of the intrinsic FFO-signal by low frequency pickup. A series of time resolved FFO-spectra gives a detailed impression of the evolution of the intrinsic FFO lineshape with time.

## I. INTRODUCTION

In the frequency range up to 1THz radio astronomical receivers nowadays are based on superconductor-insulator-superconductor (SIS) tunnel-detectors, which offer the highest possible sensitivity. Because of the high frequencies and the demanded spectral resolution of $f/\Delta f \approx 10^6$ the receivers make use of the heterodyne principle. Linewidth as well as frequency stability of the local oscillator have to be far smaller than the resolution of the employed spectrometer. Only a radiation-linewith of significantly less than 1MHz qualifies a local oscillator (LO) for the spectroscopy of radio astronomical signals at frequencies of several hundred GHz and typical 3dB-linewidths of 1MHz-10MHz.

The Flux-Flow Oscillator has developed to a promising alternative to the commonly used gunn-oscillator/multiplier combination as a local oscillator for the mm- and submm-wave region. The fabrication of the FFO-devices is fully compatible to the standard Nb/Al-$AlO_X$/Nb-technology used for SIS-mixing elements. The combination of both devices on one chip will result in highly sophisticated integrated receivers for radio astronomical applications.

In comparison with gunn-oscillator/multiplier combinations Flux-Flow Oscillators distinguishes themselves by low weight and volume, extremely low power consumption, a wide operation band and the easy frequency tuning of an ideal voltage controlled oscillator. Especially the low power dissipation and the low weight makes them very interesting candidates for satellite based heterodyne systems. For array receivers the conventional distribution of available LO-power onto the detector elements make high demands on the complex optical setup and gets increasingly difficult with growing pixel number. Here the small dimensions of the FFOs offer the possibility to integrate an own local oscillator with every SIS-junction and to separately optimize the LO-level for every element.

In this work we report on the investigation of the radiation characteristics of Flux-Flow Oscillators with regard to their radio astronomical application.

## II. Flux-Flow Oscillators

Superconducting Flux-Flow Oscillators (FFO) are traveling wave type oscillators for the mm- and submm-wave region. They are based on the unidirectional and viscous flow of magnetic flux quanta in a Josephson junction.

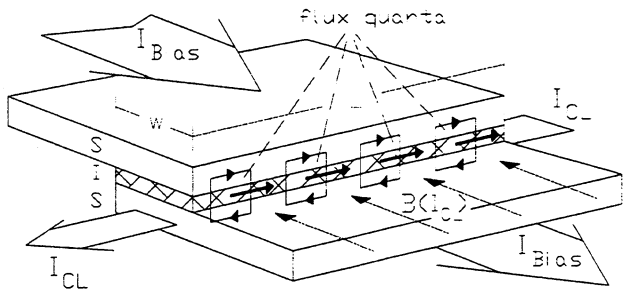


*Figure 1: Flux-Flow Oscillator. Bias current through Josephson contact drives fluxon-chain towards junction end.*

According to the Josephson penetration length $\lambda_J$ Flux-Flow Oszillators are long and even quasi-one-dimensional superconductor-insulator-superconductor (SIS) contacts (LxW≈ 400µmx3µm) with $L>>\lambda_J$ and $W<<\lambda_J$ (figure 1). A control line current $I_{CL}$ through the base electrode produces a magnetic field $B(I_{CL})$ penetrating through the barrier. It nucleates equidistant magnetic flux-quanta in the junction. The acting Lorentz force produced by the bias current $I_{Bias}$ through the element accelerates the vortices to one junction end. In balance with the quasiparticle losses this leads to a constant propagation velocity $u$ of the traveling fluxons. When the velocity of the vortex-array approaches the speed of light $\bar{c}$ in the junction this results in a steep

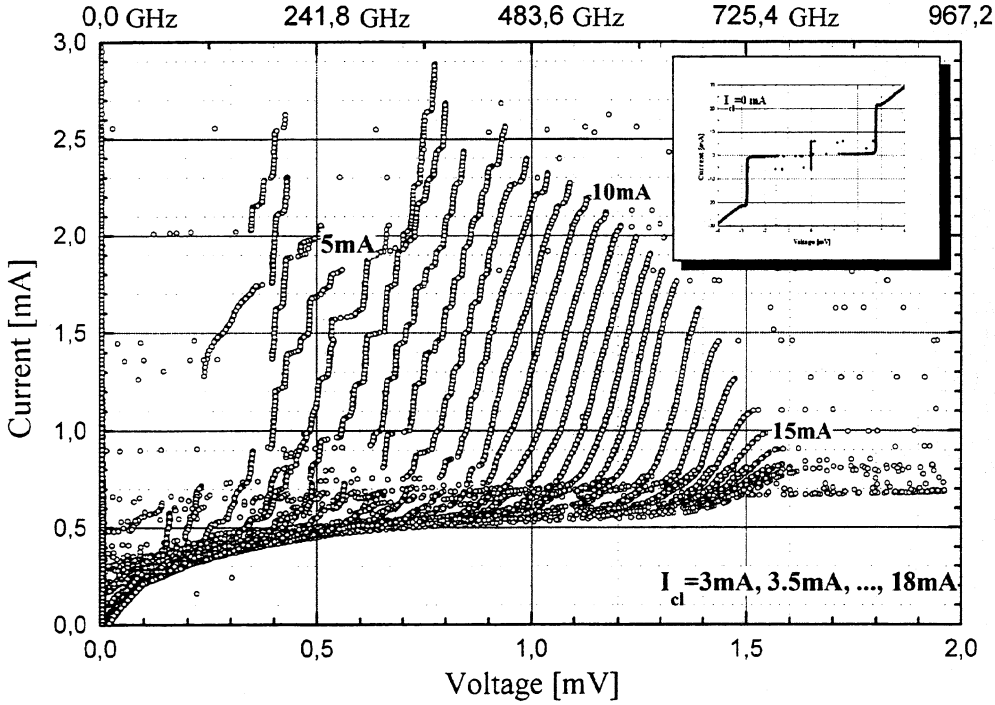


*Figure 2: Measured I-V characteristics of a FFO for different applied control current 3mA, 3.5mA...18mA. The currents correspond to a magnetic field of ~1.2G to 11.3G in the tunnel barrier or 3 to 17 trapped magnetic flux quanta respectively. The inset displays the complete I-V in absence of a control current.*

current step in the I-V characteristic of the oscillator, the so-called flux-flow step (FFS). The oscillation frequency is related to the dc-voltage drop across the junction by the Josephson relation: $f = V_{dc} / \Phi_0$ (flux quantum $\Phi_0 = h/2e$). The frequency can be continuously tuned over a wide range by changing the applied magnetic field and bias parameters. Figure 2 shows an overlay of measured I-V curves of a FFO for different applied control currents. For operating the Flux-Flow Oscillator in the 350GHz band a bias voltage of around ~0.7mV is required.

The linewidth of the emitted FFO-signal is mainly affected by the dc differential resistance $R_d$ at the bias point [1]. For low $R_d$ the linewidth is limited by external low frequency interferences (due to RF-signal pickup, hum etc.) with $\Delta f_{FFO} \sim R_d$. At high differential resistance the value of $\Delta f_{FFO}$ is determined by a superposition of shot noise and thermal noise in the junction: $\Delta f_{FFO} \sim R_d^2$. Therefore the smallest linewidth is obtained for operating the FFO on the Fiske steps (geometric resonances of oscillating fluxons in the tunnel junction) with especially low $R_d$ , which are superimposed on the FFS for $V_{bias} < 900\mu V$ in figure 2. Above that bias value the effect of Josephson self-coupling leads to an abrupt increase of the quasiparticle

damping [2] where the FFO enters the pure flux-flow regime and the linewidth increases.

## III. Measurement Setup

To investigate the FFO-linewidth and -stability in a radio astronomically interesting frequency range, a spectroscopical measurement system based on a KOSMA 345GHz SIS-mixer [3] has been set up. The FFO-radiation represents the signal to be detected whereas the mixer is operated by a PLL stabilized Gunn-oscillator as a heterodyne receiver. Mixer and Flux-Flow Oscillator are placed together in an immersion cryostat and are cooled with liquid helium. The FFO-Chip is embedded in a separate waveguide environment with integrated diagonal horn (see chapter IV). The signals are coupled to the SIS-mixer quasioptically.
Figure 3 shows an outline of the cryogenic system. The FFO-radiation is imaged by the elliptical mirror „1" and is superimposed with the local oscillator signal at the beamsplitter. The beam is then focused onto the aperture of the diagonal horn antenna and detected in the SIS-mixer.
Figure 4 depicts a photograph of the central part of the cryogenic setup. The dimensions are roughly 10cm in diameter and 30cm in height. Hidden by the sidewalls the lower level contains the beamsplitter and the two elliptical mirrors. It is solidly attached to the following level which holds SIS-mixer (left) and FFO (right). The HEMT amplifier is located on top of the setup, separated from the lower levels by teflon poles. It is connected to the SIS-mixer via a semi-rigid coax-cable and ensures an amplification of the IF-signal by 20dB at the cold stage. The majority of the optical paths of the system are capsuled in teflon. The FFO is magnetically shielded during measurements by three layers of MUMETALL®, which posses a high permeability of $\mu_r \approx 10000$ at 4.2K.

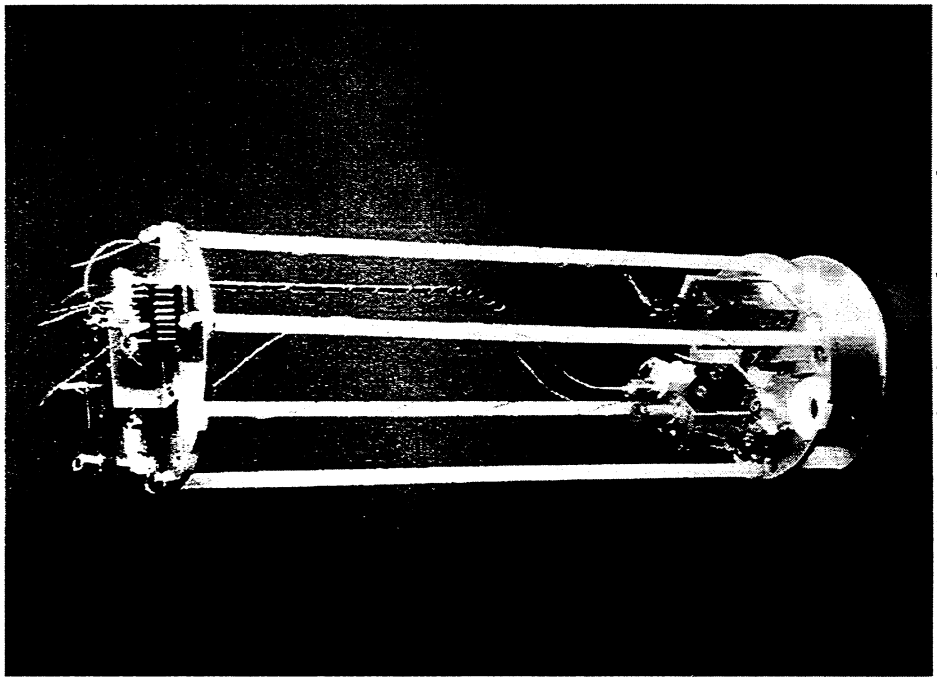

*Figure 4: Photograph of central part of measurement setup with SIS-mixer (left), Flux-Flow Oscillator block (right) and HEMT amplifier (top)*

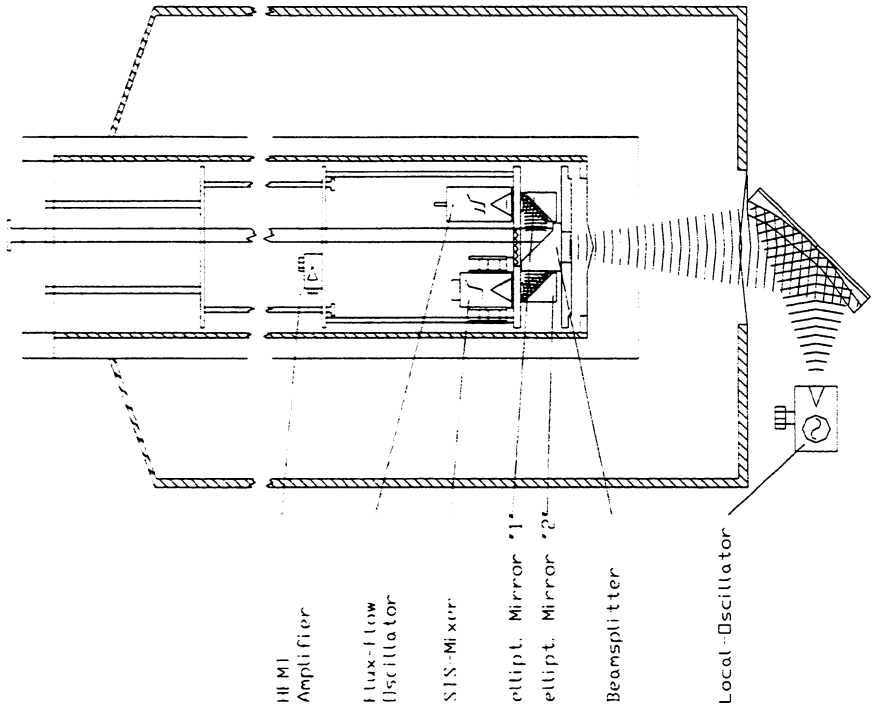


*Figure 3: Schematic diagram of the cryogenic measurement setup for the investigation of the spectral radiation properties of Flux-Flow Oscillators.*

## IV. RF-LAYOUT AND WAVEGUIDE ENVIRONMENT OF FFO-CHIP

For the detection in the SIS-mixer the FFO-radiation has to couple to the Gaussian optics of the measurement setup. For that purpose, a FFO-chip and corresponding waveguide environment for a central frequency of 350GHz have been developed.

For the RF-design of the chip the Flux-Flow Oscillator can be described in good approximation as a linear Josephson transmission line with characteristic impedance $Z_c$. Figure 5 illustrates the cross sectional view of a FFO in Nb/Al-$AlO_X$/Nb overlap geometry. The capacitive electrode overhang affects the impedance per unit length significantly. For the given values in figure 5 the characteristic impedance evaluates to $Z_c = 0.33\Omega$ [4].

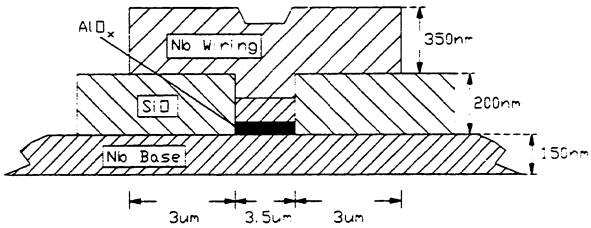


*Figure 5: Schematic cross-sectional view of FFO-layers.*

Figure 6 displays an schematic sketch of the FFO-quartz-chip. The layout uses an optimized microstrip-to-waveguide transition for 350GHz developed at MRAO University of Cambridge [5]. It has been designed for operation in low noise radio astronomical SIS-mixers and shows excellent coupling to the waveguide over a wide frequency band. The low impedance of the FFO in figure 6 is matched to a 19Ω microstrip line via a two-step impedance transformer and couples to the waveguide by the microstrip-to-finline transition. The quartz taper matches the empty to the filled waveguide. The implemented projection length of the Flux-Flow Oscillator at the junction end results in an improved bias feed and reduces the oscillator linewidth [6]. The magnetic control line current is fed through the base-electrode.

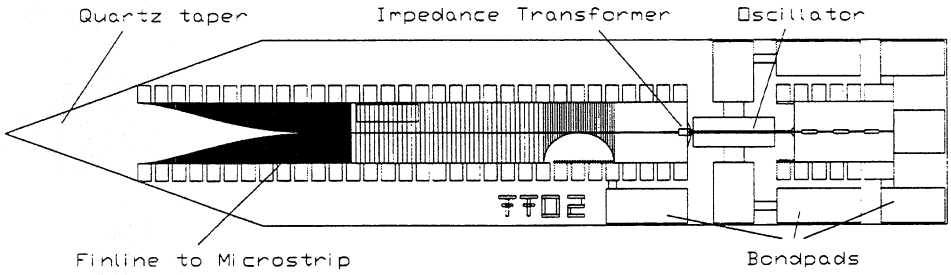


*Figure 6: Plot of FFO-chip. FFO is matched to 19Ω microstrip-line via a two-step impedance transformer. The optimized microstrip-to-finline transition [5] couples to the waveguide.*

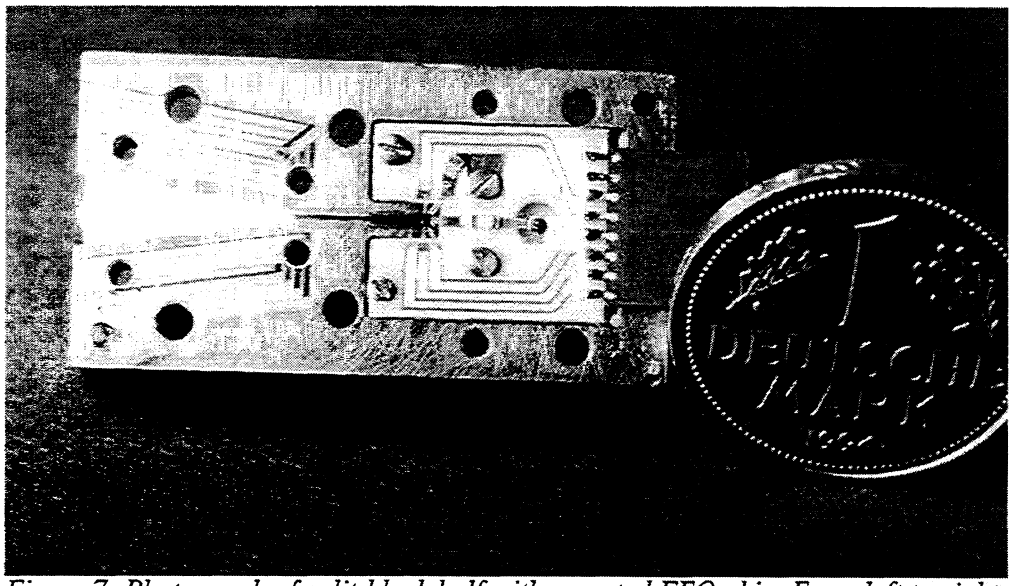

*Figure 7: Photograph of split-block half with mounted FFO-chip. From left to right: diagonal horn, waveguide, FFO-chip, SMA-connector and dc-feeds.*

The waveguide environment of the FFO-devices has been manufactured in split-block technology. Figure 7 shows a photograph of the split-block half with the mounted FFO-device. The outer dimensions of the block-half are 20mmx37.5mmx10mm (WxLxH). The FFO-chip couples to the $TEM_{01}$-mode of the waveguide which feeds the integrated diagonal horn visible at the far left in figure 7.
The FFO-elements in Nb/Al-$AlO_X$/Nb-technology were fabricated in house. The process has been proven to be fully compatible with the standard 4-layer process used for the production of SIS-mixing elements. It has already been used for the fabrication of combined SIS/FFO-devices [7].

## V. KOSMA Acousto-Optical Spectrometer

The Acousto-Optical Spectrometers (AOS) which have been developed at the University of Cologne [8] are used both as real time spectrometers and receiver backends in radio astronomy. They can easily be modified for use in time resolved spectroscopy.
Acousto-optical spectrometers are based on the diffraction of light at ultrasonic waves. A schematic drawing is given in figure 8. A RF-signal (e.g.. the 1-2GHz IF-signal coming from the SIS-mixer) drives a piezoelectric transducer, which generates an acoustic wave in a crystal. The acoustic wave modulates the refractive index of the crystal and induces a phase grating. The deflector (Bragg cell) is illuminated by a collimated laser beam. The refracted light than is collected and imaged onto a linear

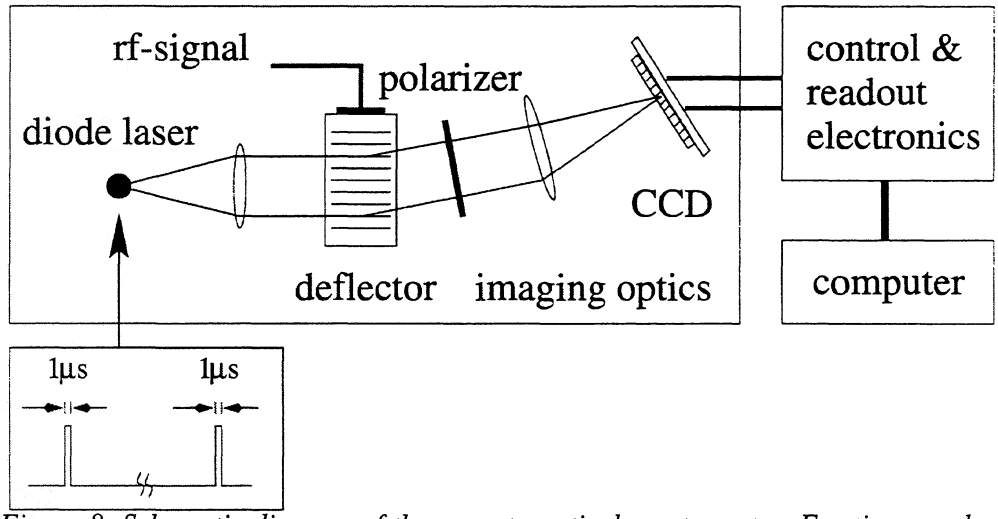


*Figure 8: Schematic diagram of the acousto-optical spectrometer. For time resolved measurements the laser diode is pulsed within 1µs to 13.5µs [9].*

diode array (CCD) in the focal plane. The angular dispersion of the diffracted light represents the true image of the IF-spectrum.

The resolution of the spectrometer depends on the aperture of the Bragg cell (i.e. dimensions of crystal), the crystal material and the imaging optics. For these measurements the KOSMA Low Resolution Spectrometer (LRS) has been available. The AOS-bandwidth of 1000MHz distributed over the 1450 pixels of the CCD result in a channel spacing of 688kHz.

In contrast to the working principle of a spectrum analyzer, the integration of a spectrum with an AOS happens for all channels simultaneously. In standard mode the laser is operated continuously. The default integration time of 10ms is given by the control electronics. The spectrum analyzer on the other hand sweeps sequentially through the frequency range and averages for a given time at every frequency point. The typical sweep time for a spectrum is 50ms to 100ms.

For time resolved measurements the laser diode of the acousto-optical spectrometer is pulsed by an external function generator with a pulse width in the range of 1µs to 13.5µs [9]. The rising edge of the pulse is synchronized with the system-intrinsic integration time of 10ms. The width of the laser pulse determines the integration time of the spectrometer in time resolved operation mode.

The transient time of the signal in the crystal limits the useful reduction of the integration time. For a measurement the phase grating has to be established in the complete Bragg cell, for which the signal has to cross the crystal. For the LRS the transient time is about 1µs. Higher frequency resolution demands a larger crystal and results in an increased transient time of the acoustic wave, about 20µs for the KOSMA High Resolution Spectrometer with its resolution-bandwidth of 30kHz.

## VI. Time Resolved Spectroscopy of FFO-Linewidth

Time resolved measurements of FFO-lineshape were taken with the modified KOSMA Acousto-Optical Low Resolution Spectrometer.

Fig. 9 shows an schematic overview of the measurement setup. The FFO-signal is superimposed with the PLL stabilized Gunn-LO-radiation and detected in the SIS-mixer. The IF-band from 1-2GHz is amplified by 20dB at the cold-stage (HEMT) and by another 40dB outside the dewar. For time resolved measurements, the laser diode of the AOS was pulsed in the range from 1μs to 13.5μs by means of a function generator. The signal is displayed simultaneously on a spectrum analyzer and the acousto-optical spectrometer. This allows direct comparison between „standard" and time resolved spectra.

Figure 10 presents a time resolved FFO-spectrum at 350GHz taken with the modified KOSMA AOS. The integration time was 1.0μs. The FFO was biased in a region with extremely low $R_d$. The linewidth of the Flux-Flow Oscillator signal is smaller than 1MHz. In this measurement the frequency-resolution is limited by the AOS channel width of 688kHz. The inset of figure 10 shows the simultaneously recorded spectrum analyzer trace (sweep time 40ms) with an FFO-linewidth of more than 20MHz.

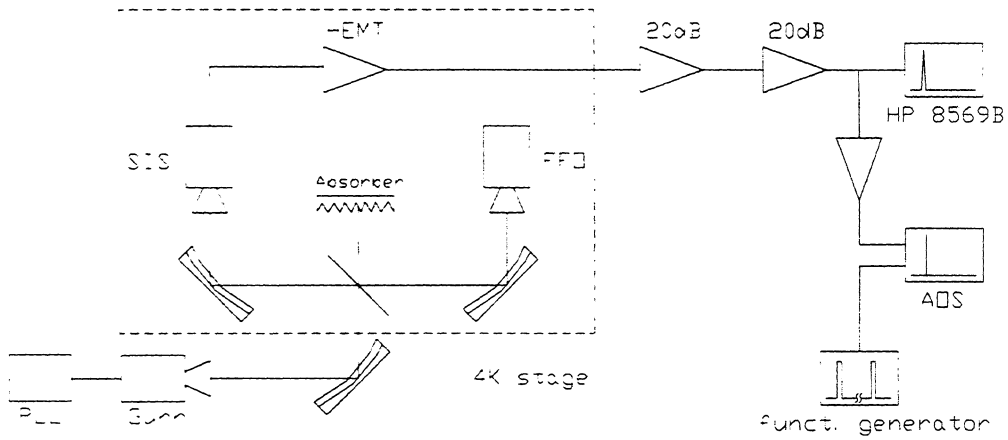


*Figure 9: Systematic setup for time resolved measurements. The FFO-signal is displayed simultaneously on a spectrum analyzer (HP 8569B) and the KOSMA AOS. The laser diode of the acousto-optical spectrometer has been pulsed by the function generator in the range from 1μs to 13.5μs.*

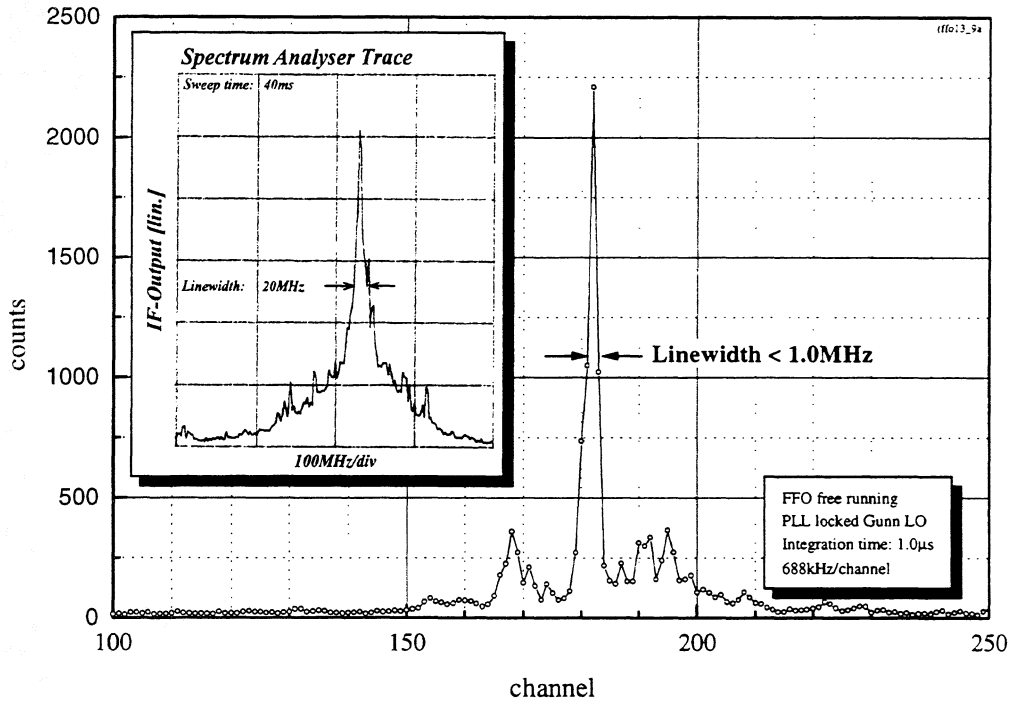


*Figure 10: Time resolved AOS-spectrum of FFO-Signal at 350GHz (1µs integration time) with a linewidth smaller than 1MHz. The inset presents a simultaneously recorded spectrum analyzer trace with a FFO-linewidth of about 20MHz (sweep time 40ms).*

The evolution of FFO lineshape with time is visible in figure 11. The spectra a)-c) have been taken in intervals of a few seconds with an integration time of 1µs each. While for the spectra a) and b) several maxima can be recognized, in spectrum c) the entire oscillator power is concentrated in a narrow peak with $\Delta f<1MHz$. The integrated intensity of the spectra varies less than 7% around the average of *8832* AOS counts. This means that the FFO-power has been constant over the period of measurement but experienced a frequency modulation on scale of the 1µs integration time. Figure 11d) illustrates the sum of spectra a)-c). The Gauss-profile fitted to the common curve has a 3dB-linewidth of 18MHz. This is in good agreement with the spectrum analyzer trace of the Flux-Flow Oscillator signal displayed in the inset of figure 11d) that shows a linewidth of 25MHz. A larger number of summarized time resolved AOS spectra should result in a further approach of the fitted linewidth to the value seen on spectrum analyzer.

The influence of the integration time on the linewidth of the measured signal can be seen in figure 12. The integration time of the acousto-optical spectrometer has been varied between 1.0µs and 13.5µs by choosing the appropriate pulse-width for operating the laser diode. The function generator limited the maximum pulse-length to

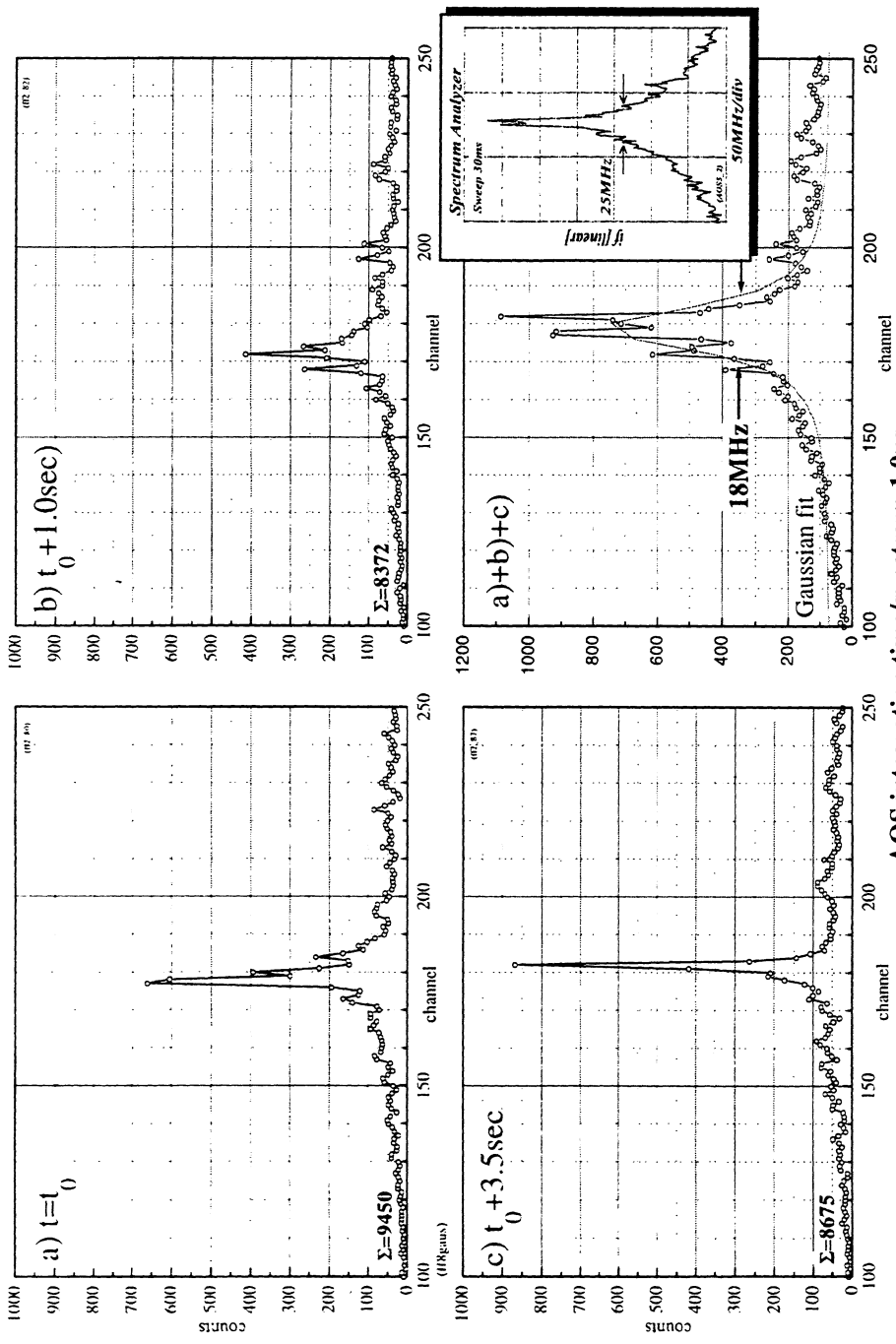


*Figure 11: Evolution of FFO-lineshape with time. a) - c) Time resolved AOS-spectra of FFO-signal with 1µs integration time taken in intervals of a few seconds. d) Sum of spectra a)-c) and fitted Gauss-profile with Δf=18MHz. The inset displays the spectrum analyzer trace taken at the same time, which shows a FFO-linewidth of Δf=25MHz.*

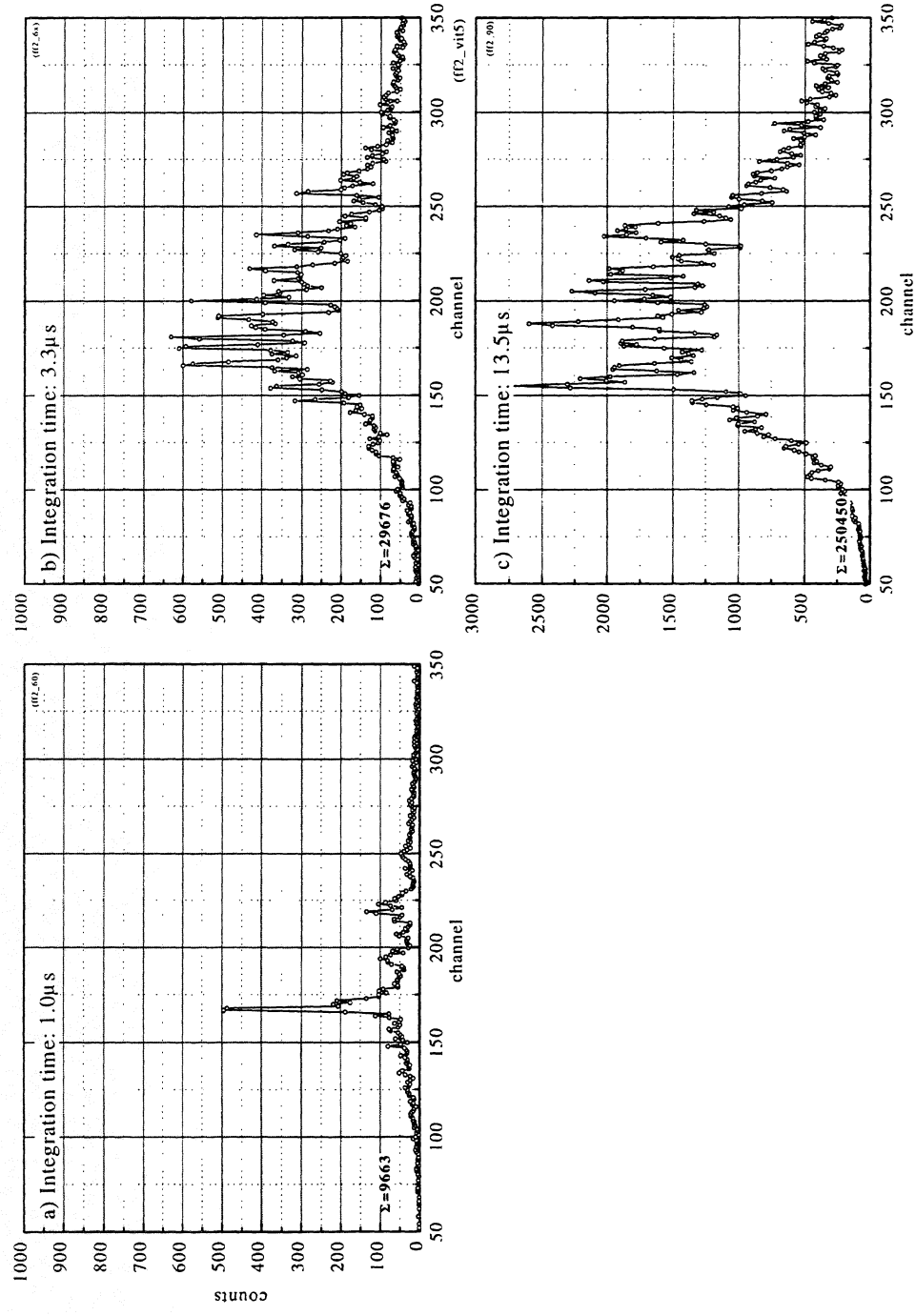


*Figure 12: AOS-spectra of FFO-signal taken with an integration time of a) 1.0µs, b) 3.3µs and c) 13.5µs respectively. Already for the integration time of 3.3µs the detected FFO-linewidth approaches the value seen on the spectrum analyzer.*

13.5μs (50kHz). The 1μs-snapshot in figure 12a) resolves a narrow FFO-signal. For the longer 3.3μs integration time (figure 12b) a significant smearing of the FFO-lineshape can be observed. The linewidth in this case corresponds to the value measured with the spectrum analyzer. A following increase of the integration time up to 13.5μs results in no further change in the detected FFO-linewidth, as can be seen in figure 12d).

As mentioned in chapter II the Flux-Flow Oscillator linewidth $\Delta f_{FFO}$ for a high differential resistance $R_d$ at its bias point is mainly given by a combination of shot noise and thermal noise, with $\Delta f_{FFO} \sim R_d^2$. Figure 13 displays a spectrum analyzer trace and a simultaneously taken AOS-spectrum of an FFO operated in that regime. A large linewidth of $\Delta f_{FFO} = 120MHz$ can be seen. The AOS integration time was 1.0μs. An improved signal/noise-ratio has been obtained by averaging over nine spectra. The linewidth at half maximum of the fitted curve is identical with the one of the spectrum analyzer trace (sweep time 40ms) in the inset of figure 13. The good agreement of measurements with short and long integration time gives evidence that the FFO-linewidth is probably determined by inherent noise processes which cannot even be resolved on the 1μs time scale.

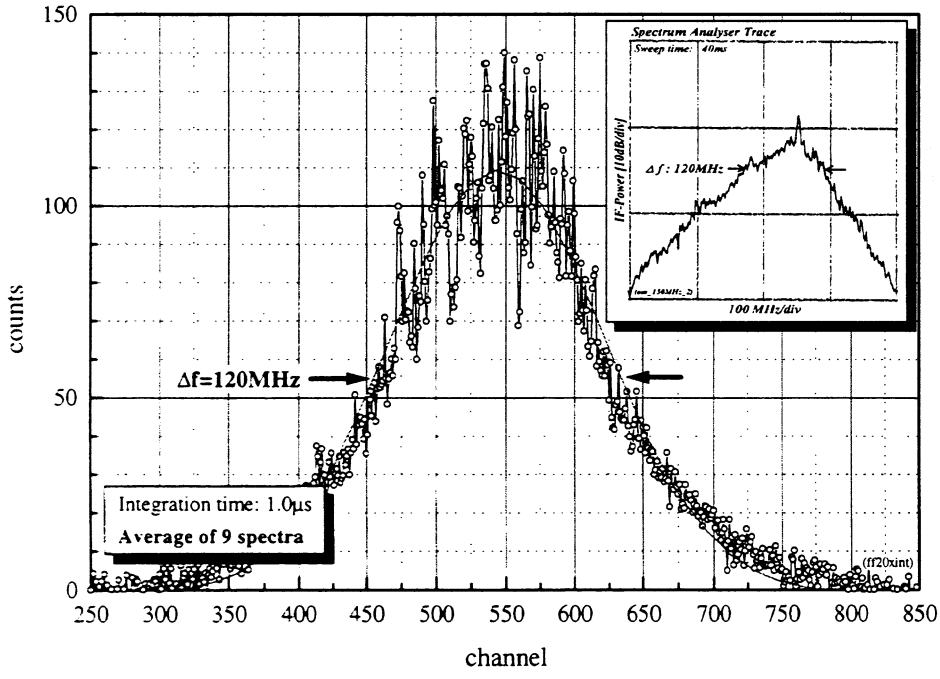


*Figure 13: Time resolved measurement (1μs integration time, average of 9 spectra) of FFO-signal: Δf=120MHz. The inset shows the spectrum analyzer trace with identical FFO-linewidth (sweep time 40ms) taken at the same time.*

## VII. Discussion of Measurements

Time resolved measurements with the modified KOSMA AOS can distinguish between the instant (intrinsic) FFO-linewidth and additional broadening due to external contributions. Low frequency interferences up to the order of the AOS-integration time can be resolved.
AOS-measurements with an integration time of 1.0μs result in a FFO-linewidth of less than 1MHz at 350GHz (figure 10). The narrow FFO-signal is modulated by external disturbances (low frequency pickup on bias feeds, hum etc.) which result in an effective signal broadening. Due to its long sweep time of 40ms the spectrum analyzer trace taken at the same time with the AOS-spectrum shows a time averaged FFO-linewidth of 20MHz.
The evolution of FFO-lineshape with time - as can be seen in the AOS-spectra in figure 11 - gives a detailed impression of the modulation of the intrinsic FFO-signal. The lineshape visible on the spectrum analyzer arises from a superposition of these time resolved spectra (figure 11d). The smeared FFO-signal for the integration time of 1μs in figure 11 and the equidistant side-peaks visible in figure 10 suggests a modulation frequency in the MHz-region.
An increase of the AOS integration time from 1.0μs up to 13.5μs leads to an increased signal-averaging. Already for a 3.3μs integration time the FFO-linewidth approaches the value seen in the spectrum analyzer measurements. This also is an indication for a pick-up frequency in the MHz-region.

## Conclusion

The determined intrinsic FFO-linewidth of less than 1MHz in principle qualifies the Flux-Flow Oscillator for use as a local oscillator in integrated radio astronomical heterodyne SIS-receivers.
An optimized RF-filtering of the bias-feeds of the Flux-Flow Oscillator and a more sophisticated magnetic shielding will result in a reduction of the effective (time averaged) FFO-linewidth and an enhanced long-term frequency stability of the oscillator signal.

For a practical integrated radio astronomical receiver it probably will be necessary to control the Flux-Flow Oscillator by a fast (>>1MHz) PLL circuit. This will further improve FFO-linewidth and -stability [1].

ACKNOWLEDGMENTS

KOSMA Superconducting Devices and Mixer developments are supported by BMBF Verbundforschung Astronomie, grants 052KV134-(6) and 053KU234-(0) and the Deutsche Forschungsgemeinschaft (DFG), grant SFB 301.

REFERENCES

[1] Valery P. Koshelets, Sergey V. Shitov, Alexey V. Shchukin, Lyudmila V. Filippenko, Pavel N. Dmitriev, Vladimir L. Vaks, Jesper Mygind, Andrey M Baryshev, Willem Luinge, Hans Goldstein, „Flux Flow Oscillators for Sub-mm Wave Integrated Receivers", Appl. Supercond. Conf. 1998, Report EQB-04, 1998

[2] V. P. Koshelets, S. V. Shitov, A. V. Shchukin, L. V. Filippenko, J. Mygind, A. V. Ustinov, „Self-pumping effects and radiation linewidth of FFO", Phys. Rev. B., Vol. 56, pp. 5572-5577, 1997

[3] S. Haas, „Low noise fixed-tuned SIS mixer for astronomical observations in the submm wave region", Ph.D. thesis, University of Cologne, 1998

[4] C. E. Tong, R. Blundell, „ Sub-millimeter distributed quasiparticle receiver employing a non-linear transmission line", 7th Int. Symp. on Space Terahertz Tech., Charlotteville, 1996

[5] G. Yassin, S. Withington, R. Padman, „Electromagnetic Analysis of Finline Mixers", University of Cambridge, Department of Physics, internal report No. 2018, 1997

[6] T. Nagatsuma, K. Enpuku, K. Sueoka, K. Yoshida, F. Irie, „Flux-flow-type Josephson oscillator for millimeter and submillimeter wave region III. Oscillation Stability", J. Appl. Phys., Vol. 58, No. 1, 1985

[7] U. Müller, „Charakterisierung supraleitender Flux-Flow Oszillatoren für den Einsatz als Lokaloszillatoren in SIS-Heterodynempfängern", Ph.D. thesis, University of Cologne, in preparation

[8] R. Schieder, V. Tolls, G. Winnewisser, „The Cologne Acousto Optical Spectrometers", Exp. Astron., Vol. 1, 1989

[9] O. Siebertz, University of Cologne, 1998

damage threshold, the increase of the laser power reflects directly the THz output power. The increase of the laser power density may also contribute to the output power improvement, because the output saturation effect could be reduced by increasing the laser power density, as described above. This can be done by shortening the active area length (laser spot size), and it contribute to reduce the stripline loss, too. Another way is increasing the photoconductivity by narrowing the stripline gap. If the 1-μm gap device is used, the output power increases by a factor of 4, though the ohmic loss would increase and cancel the power gain a little. In addition, the radiation loss can be reduced by narrowing the total stripline width, and the substrate absorption can be eliminated by employing a silicon substrate. The silicon based photomixer offers additional benefit of high power handling capability.[5] By combining these power gain factors, one order of magnitude output power improvement would be achieved.

## Acknowledgment

The authors would like to thank T. E. Turner in the Microelectronics Device Laboratory at JPL for device fabrication. This research was sponsored by the Jet Propulsion Laboratory, California Institute of Technology, and the National Aeronautics and Space Administration. The work performed at UCSB was supported by the Center for Nonstoichiometric III-V Semiconductors.

## References

[1] E. R. Brown, F. W. Smith, and K. A. McIntosh, *J. Appl. Phys.*, **73**, 1480 (1993).

[2] E. R. Brown, K. A. McIntosh, F. W. Smith, K. B. Nichols, M. J. Manfra, C. L. Dennis, and J. P. Mattia, *Appl. Phys. Lett.*, **64**, 3311 (1994).

[3] K. A. McIntosh, E. R. Brown, K. B. Nichols, O. B. McMahon, W. F. DiNatale, and T. M. Lyszczarz, *Appl. Phys. Lett.*, **67**, 3844 (1995).

[4] S. Matsuura, M. Tani, and K. Sakai, *Appl. Phys. Lett.*, **70**, 559, (1997).

[5] S. Verghese, K.A. McIntosh, and E.R. Brown, *IEEE Trans. Microwave Theory and Tech.*, **45**, 1301 (1997).

[6] P. Chen, G. A. Blake, M. C. Gaidis, E. R. Brown, K. A. McIntosh, S. Y. Chou, M. I. Nathan, and F. Williamson, *Appl. Phys. Lett.* **71**, 1601 (1997).

[7] S. Matsuura, P. Chen, G. A. Blake, J. C. Pearson, and H. M. Pickett, , *IEEE Trans. Microwave Theory and Tech.*, (1999), in press.

[8] L. Y. Lin, M. C. Wu, T. Itoh, T. A. Vang, R. E. Muller, D. L. Sivco, and A. Y. Cho, *IEEE Phton. Technol. Lett.*, **8**, 1376 (1996).

[9] Y. -J. Chiu, S. B. Fleischer, and J. E. Bowers, *IEEE Phton. Technol. Lett.*, **10**, 1021 (1998).

[10] S. Matsuura, P. Chen, G. A. Blake, J. C. Pearson, and H. M. Pickett, Int. *J. of Infrared and Millimeter Waves*, **19**, 849 (1998).

[11] S. Verghese, private communication.

[12] K. C. Gupta, R. Garg, and R. Chadha, *Computer-aided Design of Microwave Circuits*, (Artech House, Norwood, MA, 1981), p. 72.

[13] D. B. Rutledge, D. P. Neikirk, and D. P. Kasilingam, in *Infrared and Millimeter Waves*, edited by K. J. Button (Academic Press, New York 1983), Vol. 10, p. 1.